Noncovalent Binding of a Reaction Intermediate by a Designed Helix-Loop-Helix Motif—Implications for Catalyst Design

Malin Allert[b] and Lars Baltzer*[a]

In our search for a catalyst for the transamination reaction of aspartic acid to form oxaloacetate, twenty-five forty-two-residue sequences were designed to fold into helix-loop-helix dimers and form binding sites for the key intermediate along the reaction pathway, the aldimine. This intermediate is formed from aspartic acid and the cofactor pyridoxal phosphate. The design of the binding sites followed a strategy in which exclusively noncovalent forces were used for binding the aldimine. Histidine residues were incorporated to catalyse the rate-limiting 1,3 proton transfer reaction that converts the aldimine into the ketimine, an intermediate that is subsequently hydrolysed to form oxaloacetate and pyridoxamine phosphate. The two most efficient catalysts, T-4 and T-16, selected from the pool of sequences by a simple screening procedure, were shown by CD and NMR spectroscopies to bind the aldimine intermediate with dissociation constants in the millimolar range. The mean residue ellipticity of T-4 in aqueous solution at pH 7.4 and a concentration of 0.75 mM was $-18\,500\ deg\,cm^2\,dmol^{-1}$. Upon addition of 6 mM L-aspartic acid and 1.5 mM pyridoxal phosphate to form the aldimine, the mean residue ellipticity changed to $-19\,900\ deg\,cm^2\,dmol^{-1}$. The corresponding mean residue ellipticities of T-16 were $-21\,200\ deg\,cm^2\,dmol^{-1}$ and $-24\,000\ deg\,cm^2\,dmol^{-1}$. These results show that the helical content increased in the presence of the aldimine, and that the folded polypeptides bound the aldimine. The ^1H NMR relaxation time of the imine CH proton of the aldimine was affected by the presence of T-4 as was the ^{31}P NMR resonance linewidth. The catalytic efficiencies of T-4 and T-16 were compared to that of imidazole and found to be more than three orders of magnitude larger. The designed binding sites were thus shown to be capable of binding the aldimine in close proximity to His residues, by noncovalent forces, into conformations that proved to be catalytically active. The results show for the first time the design of well-defined catalytic sites that bind a reaction intermediate with enzyme-like affinities under equilibrium conditions and represent an important advance in de novo catalyst design.

Introduction

New enzymes can be envisioned to be of great fundamental as well as of great practical value, but their design from scratch remains a demanding endeavour. Although several enzymatic reactions appear to be fairly well understood, introduction of the corresponding, or new, catalytic functions into designed or re-engineered protein scaffolds at the level of refinement that characterises native enzymes, is not easily achieved. Several polypeptide model systems,[1–3] catalytic antibodies[4–7] and re-engineered enzymes[8, 9] have been designed and shown to exhibit properties that partly mimic those of native enzymes, for example, they show large rate enhancements, follow saturation kinetics and discriminate between substrates. The analysis of the properties of these molecules has provided much insight into catalysis and important steps have been taken towards tailor-made enzymes. However, an understanding of how to design new enzymes from scratch has not emerged.

The de novo design of proteins provides the opportunity to test fundamental functions in model systems that do not have the complexity of native proteins.[2, 3, 10–20] Designed catalysts have been reported for decarboxylation,[1, 21, 22] chemical ligation,[23–27] amidation,[28] hydrolysis,[28–32] transesterification[29] and transamination reactions.[33] In the majority of these reactions,

saturation kinetics were observed under turnover conditions, the hallmark of native enzymes, and rate enhancements of more than three orders of magnitude were achieved.[1, 22–26, 29] It is fair to say that the reactions catalysed so far in model systems are less complex than those that normally take place in the living cell. The studied reactions go through intermediates that are covalently linked to the catalyst, or have rate-limiting steps early in the reaction pathway, and bypass one aspect of biocatalysis that is especially difficult to mimic, namely the specific but differential binding of substrates, several intermediates and

[a] *Prof. L. Baltzer*
Department of Chemistry
Linköping University, 581 83 Linköping (Sweden)
Fax: (+46) 1312-2587
E-mail: Lars.Baltzer@ifm.liu.se

[b] *Dr. M. Allert*
Department of Chemistry
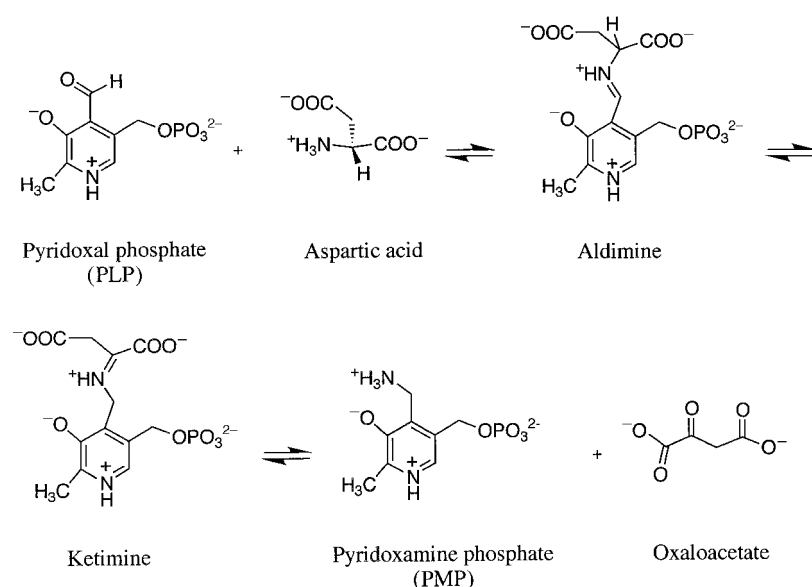*Organic Chemistry, Göteborg University*
41296 Göteborg (Sweden)

transition states by noncovalent forces. The acylated histidine side chain in His-mediated ester hydrolysis[32] and the imines in oxaloacetate decarboxylation[1, 22] are illustrative examples of intermediates that are covalently bound to the catalyst. In the self-replication of helical peptides, catalysis has been achieved by bringing the reactants together for the first and rate-limiting bond-forming step and thus the binding of subsequent intermediates along the reaction pathway did not affect the catalytic efficiency.[23–26] Since multistep reactions with clearly identifiable intermediates are the rule rather than the exception in enzyme catalysis, the development of an understanding of how to construct sites that bind small molecules represents an important goal in catalyst design.

An important reaction in biocatalysis is the transamination of amino acids to form the corresponding α-keto acids (Scheme 1).[34–36] The reaction is reversible and is the key sequence in the biosynthesis of the naturally occurring amino acids. It is of commercial value in the production of artificial amino acids by technological fermentation processes. Imines derived from the pyridoxal phosphate aldehyde, the so-called aldimines, form the first two observable intermediates in the enzymatic transformation of an amino acid. In reactions catalysed by aspartate transaminases, the first aldimine is formed from the cofactor pyridoxal phosphate and a lysine residue in the active site. Upon introduction of an amino acid into the binding pocket, the second aldimine is formed as the amino group of the amino acid replaces the lysine residue in an exchange reaction.[35, 36] The transamination reaction is based on the "electron sink" capacity of the cofactor pyridoxal phosphate and the cofactor – amino-acid intermediates are bound to the enzyme by noncovalent forces.

The aldimine is converted to the ketimine in a 1,3 proton transfer reaction that under nonenzymatic conditions is the rate-limiting step. This aldimine intermediate is a long-lived species that is formed rapidly but consumed slowly. The reaction is reversible and the equilibrium favours the aldimine strongly over the ketimine. A central concept in the design of catalysts for the transamination of amino acids is the construction of a binding site for the aldimine in which residues that reside in the site can catalyse the proton transfer reaction by cooperative general-base and general-acid catalysis. The catalyst – aldimine complex must be sufficiently populated for proton-transfer catalysis to be efficient, and the aldimine must be bound within bond-forming distance of the catalytically active base. Our long-term aim is to develop novel catalysts for the transamination reaction in the biosynthesis of artificial amino acids. The transformation of aspartic acid to form oxaloacetate is of special interest as Asp is readily available at low cost and is an attractive source of amino groups. The design of a binding site for the aldimine from L-Asp was therefore selected as the critical test of our ability to bind a long-lived intermediate in a catalytic site and to design catalysts for complex reactions from scratch. Catalysts for the trans-amination reaction have previously been successfully designed; derivatives of pyridoxal phosphate were covalently linked to a naturally occurring lipid-binding protein (adipocyte lipid-binding protein)[37–39] and to a designed 23-residue miniprotein.[33, 40] We now report that we have designed a number of helix-loop-helix dimers capable of binding the aldimine intermediate formed in pyridoxal phosphate mediated amino acid trans-amination exclusively by noncovalent forces. Weak interactions between the proteins and the aldimine were observed by NMR and CD spectroscopies. The precision of the binding was probed by the incorporation into the protein scaffold of groups capable of carrying out the 1,3 proton transfer reaction to form the reaction products. This is the first report of a de novo designed protein that is capable of binding a reaction intermediate of low molecular weight exclusively by noncovalent forces and represents an important step towards the design of catalysts for multistep reactions.
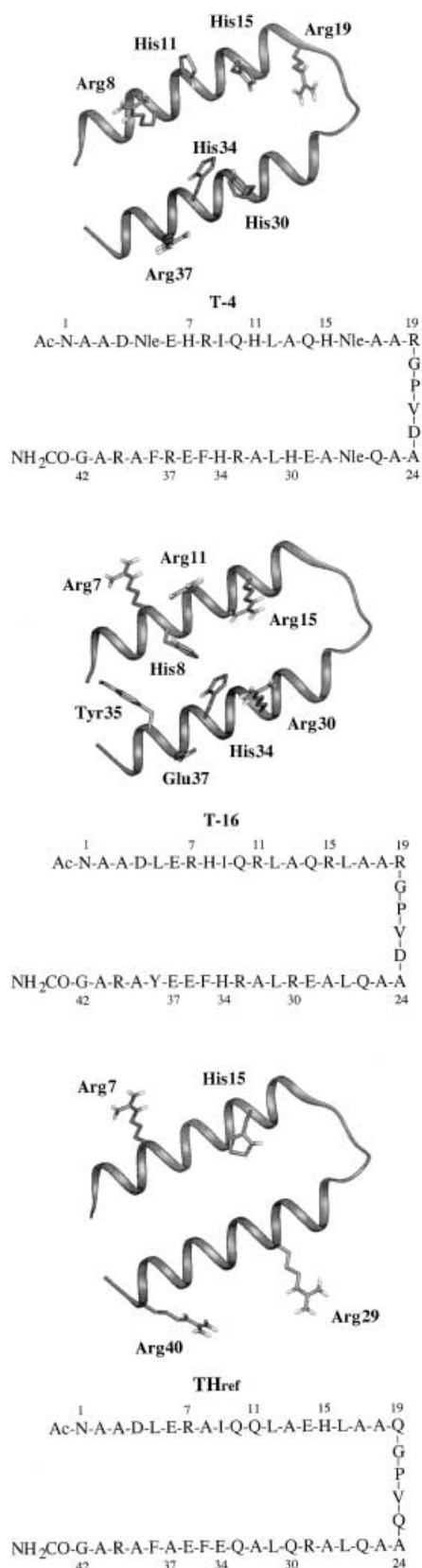
Results

Design and characterisation of the four-helix bundle motif

Twenty-five sequences (see the Supporting Information) were designed to form helix-loop-helix motifs and dimerise into four-helix bundles. Residues were introduced at the surface of the folded motifs in a systematic fashion to bind the aldimine intermediate and to catalyse its conversion to the ketimine (Scheme 1). Two sequences, T-4 and T-16, (Figure 1) were selected for further investigations with regards to their capacity for binding the aldimine intermediate, based on their ability to catalyse the transamination reaction. For comparison with T-4 and T-16, a reference sequence, Thref (Figure 1), was designed to fold into a four-helix bundle motif

Scheme 1. *The mechanism of the transamination reaction. The amino group of the amino acid reacts with the aldehyde group of pyridoxal phosphate to form the aldimine. A 1,3 proton transfer transforms the aldimine into the ketimine and the ketimine is hydrolysed to form oxaloacetate and pyridoxamine phosphate. The reaction sequence is reversible.*

L. Baltzer and M. Allert

Figure 1. *The modelled structures and the amino acid sequences of (a) T-4, (b) T-16 and (c) Thref. The one-letter code is used to denote the amino acid residues in the sequences, with norleucine given as Nle. Only the side chains of the residues designed to form the binding sites are shown and only the monomer of the peptide is represented, for clarity of presentation.*

into which Arg and His residues were introduced at different positions from those used in T-4 and T-16. The amino acid sequences were based on those of the de novo designed template polypeptide SA-42[41, 42] and the polypeptides KO-42, LA-42b and KA-I[29, 43] developed from SA-42. In short, the polypeptides were designed to fold into two amphiphilic helical segments connected by a short loop. The amino acid residues in the helical segments were selected according to their propensities for helix formation. Capping residues and charged residues capable of salt bridge formation and of helical dipole stabilisation were introduced to increase the helical stability.[11, 44] Nonpolar residues were incorporated into the sequence to form complementary shaped hydrophobic surfaces upon folding and to drive the formation of the helix-loop-helix hairpin and its dimerisation. The design of the four-helix bundle motif is conveniently described in terms of the heptad repeat pattern ($abcdefg$)$_n$ (Figure 2).[11] In the antiparallel helix-loop-helix dimer formed from SA-42 the residues in the a and d positions form the hydrophobic core, those in the c and g positions form the "top" and "bottom" surfaces of the dimer and the residues in the b and e positions control dimerisation.
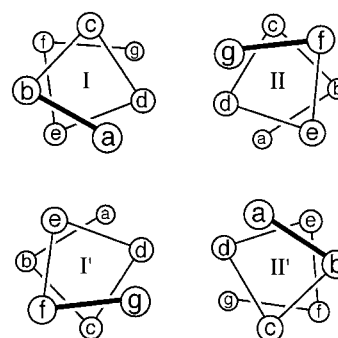
Figure 2. *Schematic representation of the heptad repeat pattern for antiparallel helix-loop-helix dimers. The residues in the* a *and* d *positions form the hydrophobic core, those in the* g *and* c *positions form the exposed surface of the motif and the residues in the* b *and* e *positions are localised at the dimer interface.*

The sequences SA-42,[41, 42] KO-42,[29] LA-42b[43] and KA-I[45] were previously characterised extensively by NMR and CD spectroscopies, and the states of aggregation of SA-42 and KO-42 were analysed by analytical ultracentrifugation. The sequences were all shown to adopt hairpin helix-loop-helix motifs that dimerise in an antiparallel fashion to form the four-helix bundle structure. The a and d residues of the hydrophobic core were essentially identical for all the sequences, with the exception that the α-amino isobutyric acid (Aib) residues of SA-42 and KO-42 were replaced by alanine residues in LA-42b and KA-I. The b and e positions were also preserved throughout, whereas residues at the c and g positions were introduced in each sequence according to the purpose for which the sequence was designed. There was no evidence to suggest that changes in c and g residues changed the overall folds.

High-resolution NMR spectroscopy structures were not obtained as the dimers had partly disordered hydrophobic cores and their resonances were in fast exchange on the NMR time

scale, which results in time-averaged NOEs that could not be used in three-dimensional structure calculations. The helical segments could, however, be identified and so could the antiparallel fold of the helix-loop-helix dimers (Figure 2), which was the only fold observed in spite of the fact that several alternative four-helix bundle folds are possible. The results were in agreement with kinetic data from the hydrolysis of *p*-nitrophenyl esters, where the introduction of an arginine and a lysine residue into the *c* and *g* positions in helix I increased the reactivity of the cooperative HisH+-His site in the *d* and *g* positions in helix II. Cooperativity between *c*, *d* and *g* residues in helix I and helix II is only possible in the fold shown in Figure 2.[30, 46] The sequences reported herein were designed according to the same principles, with the hydrophobic core residues remaining essentially the same as the sequences described above. We assumed that the similarity with the sequences SA-42, KO-42, LA-42b and KA-I would mean that the sequences reported here would adopt the same fold.

Detailed NMR analyses of the solution structures of the peptides presented herein were therefore not carried out, but the temperature dependence of the ¹H NMR spectrum of T-16 in the interval between 278 and 318 K was determined (Figure 3). One-dimensional NMR spectra are informative because the folded polypeptides are macromolecules in chemical exchange between several conformers at an intermediate rate on the NMR time scale, as discussed previously.[41, 42] The observed temperature dependence of the T-16 spectrum showed that the sequence is in fast exchange on the NMR time scale but approaches coalescence as the temperature is decreased. This is in agreement with the assumption that the fold and state of aggregation of T-4 and T-16 are similar to those of the parent peptides.

The mean residue ellipticity of a polypeptide at 222 nm is a qualitative measure of structure and of dimer formation. A large negative value at high peptide concentration shows that the peptide has a high helical content, and a small negative value of peptide ellipticity at low concentration shows that the peptide is largely unfolded at that concentration and is dependent on aggregation for structure formation.[41, 42] The mean residue ellipticities of the twenty-five sequences at 222 nm ranged from $-15\,000$ to $-26\,000$ deg cm² dmol⁻¹ at pH 7.4, 0.5 mM, and room temperature, which is well within the range of previous designs based on the SA-42 sequence. The concentration dependence of the mean residue ellipticities of T-4 and T-16 were determined (Figure 4) and demonstrated that the peptides were involved in monomer-dimer equilibria. It cannot be excluded that they are also involved in higher-order equilibria at high peptide concentrations, as observed previously for SA-42 at 5 mM.

Design of binding sites for the aldimine intermediate

The aldimine intermediate is highly negatively charged at neutral pH. The two carboxylic acid residues originating from aspartic acid are almost completely dissociated above pH 5 and of the two pK_a values of the phosphate monoester, one is probably less than 2 whereas the other is 6.3.[47] The hydroxy group also has a low pK_a value and is fully dissociated under the
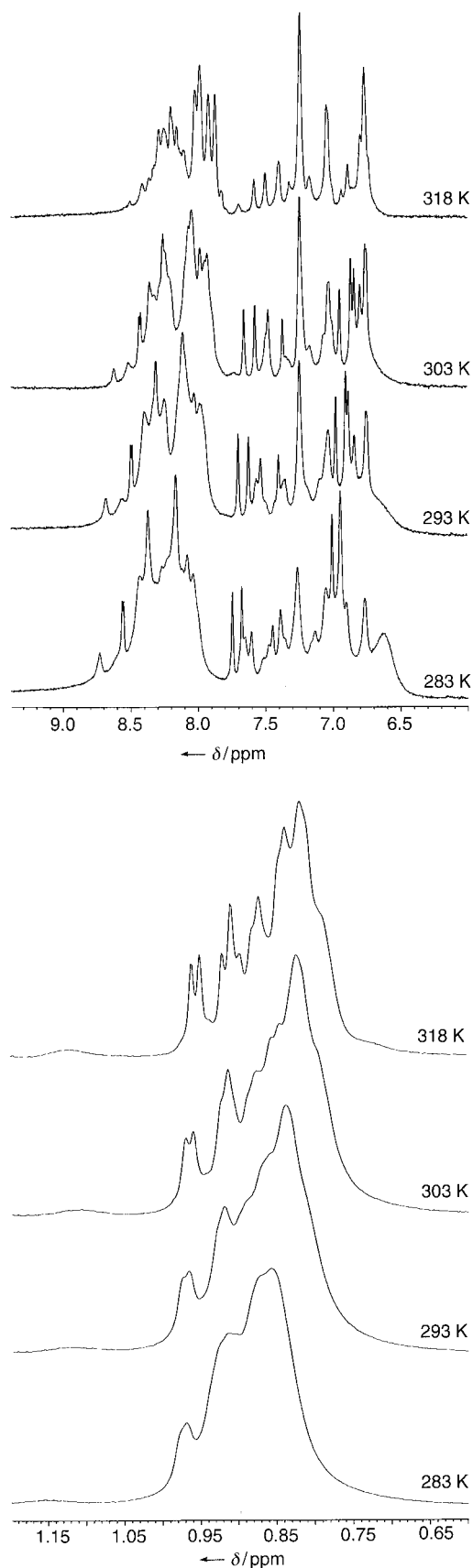
Figure 3. a) The amide region and (b) the methyl region of the ¹H NMR spectrum of T-16 as a function of temperature. The concentration of T-16 was 0.5 mM in phosphate buffer solution (90 mM)/D₂O (90:10) at pH 5.5 and 278 – 323 K.
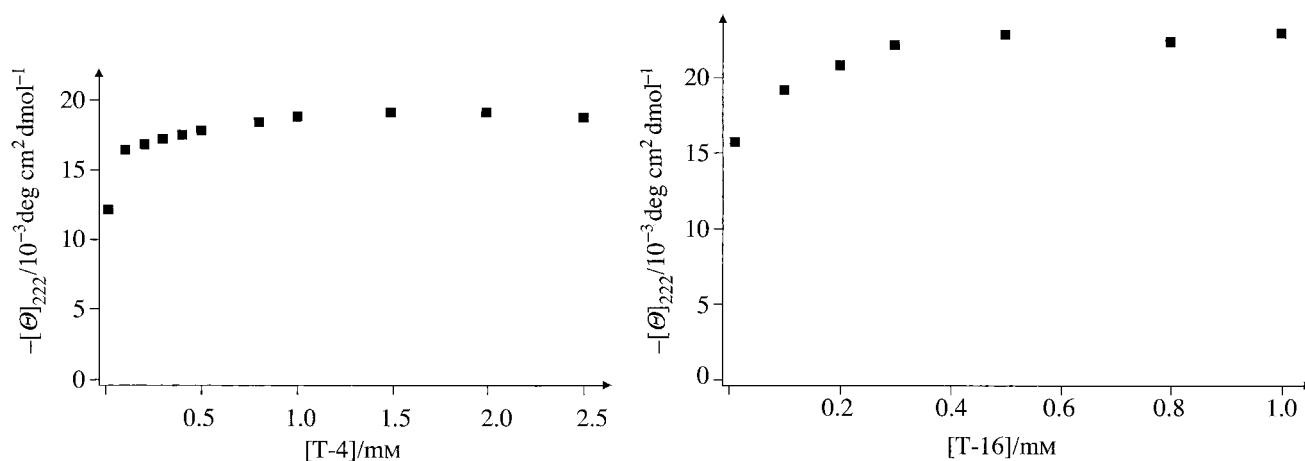
Figure 4. *The concentration dependence of the mean residue ellipticity at 222 nm, Θ_{222}, of (a) T-4 , (b) T-16 in aqueous solution at pH 7.5 and room temperature.*

experimental conditions. The nitrogen atom of the pyridine ring is partly protonated since the aldimine pyridinium ion has a pK_a of 6.6, whereas the imine nitrogen atom is completely protonated, with a pK_a above 10. The pK_a values show that the aldimine carries a total of almost four negative charges at pH 7.4 and more than two at pH 5.5. The variation of charge with pH value was exploited in the study of aldimine binding. At higher pH values, the aldimine was expected to bind better to the catalyst as a result of the larger total negative charge on the aldimine. At lower pH values, catalysis was expected to be more efficient since the pyridinium ion would be formed to a larger degree and the protonated and unprotonated states of the His residues were expected to be approximately equally probable. Binding sites on the surface of the folded motif were designed to bind the aldimine and ketimine intermediates by introducing positively charged arginine residues to interact with the negatively charged substituents through electrostatic interactions and hydrogen bonding. Arginine residues are known to bind negatively charged phosphate groups and in the aspartate transaminases arginine residues stabilise the two carboxylate groups of the aspartate residue.[48, 49] Arginine residues were incorporated at the *c* and *g* positions on the surface of the peptides in geometries that were expected to put these residues simultaneously within range of several charge complementary substituents of the intermediates. In T-4, arginine residues were introduced at positions 8, 19, 33 and 37 (Figure 1 a) and in T-16 they were incorporated in positions 7, 11, 15, 30 and 33 (Figure 1 b). Lysine residues were also used to form binding sites for the aldimine but were found to favour the formation of imines with the cofactor pyridoxal phosphate rather than binding the aldimine formed from the amino acid in surface exposed sites and were not used further. Lysine-containing sequences were shown previously to have a high propensity for imine formation with the pyridoxal phosphate cofactor when flanked by arginine residues.[50]

In naturally occurring transaminases, lysine residues catalyse the 1,3 proton transfer reaction of the aldimine-to-ketimine transformation.[48, 49, 51] In aspartate transaminase, a lysine residue in the active site binds the pyridoxal phosphate through an

imine linkage and catalyses the 1,3 proton transfer as it is released upon introduction of the amino acid substrate. For the reasons presented above, lysine residues were not used for this purpose in the catalysts reported here, although they might be considered in a more constrained binding site. Histidine residues were instead introduced into the T-4 and T-16 sequences in positions where they were in close proximity both to the α proton of the aspartate residue of the aldimine, and to the CH proton of the imine (Scheme 2). The designed reactive site of T-4 was based on four closely grouped histidine residues in positions 11, 15, 30 and 34 and that of T-16 contained two histidine residues in positions 8 and 34. Several histidine residues were incorporated in T-4 as part of the design strategy because of the difficulties involved in accurately predicting the position of the aldimine in a designed binding site. In T-16, histidine residues were incorporated in a more minimalistic way. The design of T-16 was inspired to a higher degree by the native enzyme aspartate transaminase than that of T-4 and amino acids were introduced into the sequence of T-16 that are known to stabilise the complex between this enzyme and the aldimine intermediate. A glutamic acid residue was introduced at position 37 of T-16 for
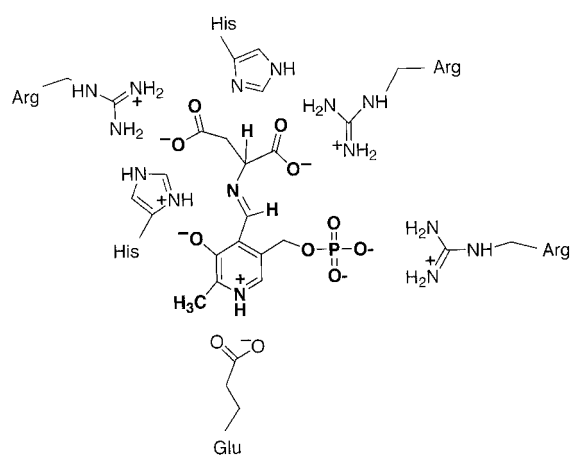
Scheme 2. *A schematic representation of the designed interactions between the aldimine intermediate and the binding residues in the folded polypeptide motif.*
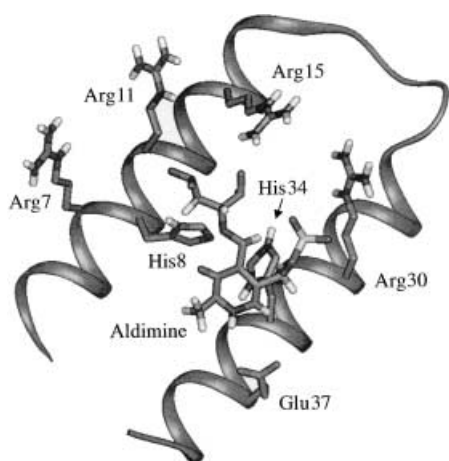
Figure 5. *Modelled structure of the complex formed between T-16 and aldimine. Only side chains designed to be involved in binding the intermediate are shown.*

possible stabilisation of the pyridinium ion and a tyrosine residue at position 38 for the possible interaction with the hydroxy group of the pyridoxal phosphate (Scheme 2). The optimal pH value for catalysis depends on the pK_a value of the His residues as the 1,3-proton-transfer reaction requires a base as well as an acid. If histidine residues are to act as acid and base the optimal pH value is one where there are equal proportions of protonated and unprotonated His residues, that is, the pH value should equal that of the histidine pK_a. An illustration of the aldimine bound to the designed binding site of T-16 is shown in Figure 5.

The equilibrium constant for aldimine formation and the assignment of the NMR spectrum

The interactions between the aldimine and the designed binding sites of T-4 and T-16 were monitored by NMR and CD spectroscopies. The reaction between pyridoxal phosphate and aspartic acid to form the aldimine is reversible and all three species coexisted in solution under the experimental conditions. To control the concentration of the aldimine, the equilibrium constant for aldimine formation was estimated from the integrals of the resonance signals of the participating species. In the ^{1}H NMR spectrum of L-aspartic acid in H_2O/D_2O (90:10) at pH 7.4 and room temperature, the resonance at 3.90 ppm was assigned to the α proton according to its chemical shift and multiplicity. The two resonances at 2.68 and 2.82 ppm were assigned to the β protons in the same way. In the spectrum of pyridoxal phosphate there were only four resonances and they were assigned according to their chemical shifts and their integrals.[47] The resonance at 10.45 ppm is from the single aldehyde

proton. The resonance at 7.79 ppm is from the single proton in the aromatic ring, that at 5.11 ppm is from the methylene protons adjacent to the phosphate group and the resonance at 2.50 ppm is that of the methyl group. Upon mixing L-aspartic acid and pyridoxal phosphate, the intensity of the aldehyde proton was reduced and a new set of resonances appeared, which were assigned to the aldimine (Figure 6).[47] The resonance at 7.65 ppm was tentatively assigned to the aldimine aromatic ring proton because of the similarity between its chemical shift and that of the ring proton of pyridoxal phosphate. The resonance at 4.92 ppm arises from the aldimine methylene group adjacent to the phosphate. The aldimine methyl group was found at 2.43 ppm, and the resonance of the carbon-bound imine proton appeared at 8.92 ppm (Figure 7). The resonances of the α and β protons of the aspartic acid moiety were shifted relative to those seen for free L-Asp. The β protons were shifted only slightly to 2.96 and 2.91 ppm and the α proton was shifted to 4.61 ppm. The dissociation constant of the aldimine was estimated from the magnitude of the integral of the cofactor aldehyde proton resonance at 10.45 ppm and that of the imine proton of the aldimine at 8.92 ppm. The spectrum was recorded
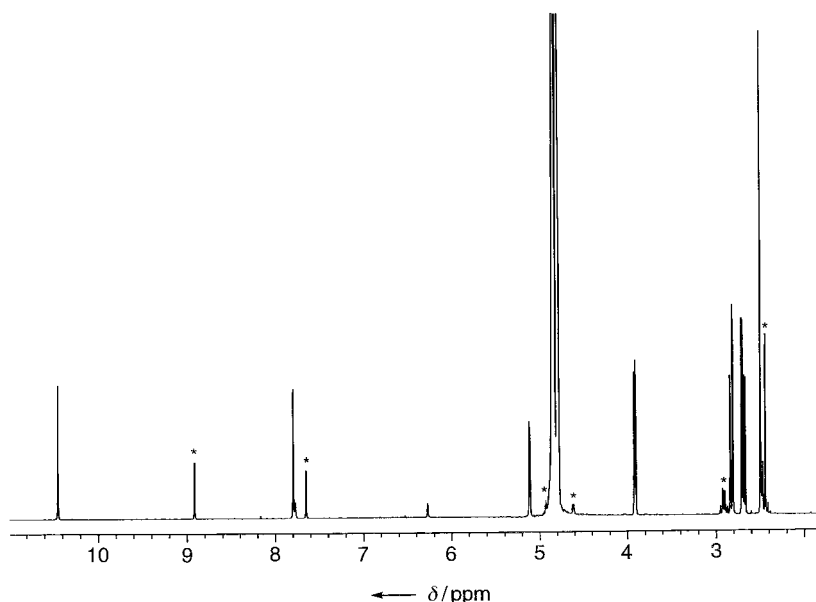
Figure 6. *The ^{1}H NMR spectrum of the reaction mixture of pyridoxal phosphate (5 mM) and L-Asp (10 mM) in phosphate buffer solution (50 mM)/D_2O (90:10) at pH 7.4 and 298 K.*
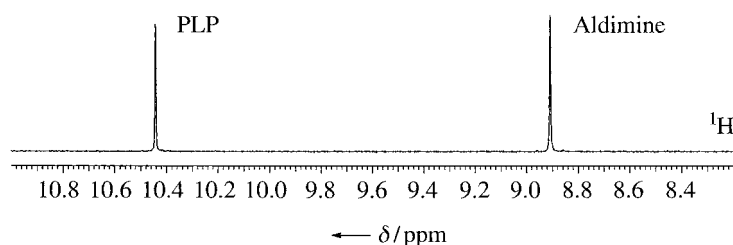
Figure 7. *Part of the ^{1}H NMR spectrum of an aqueous solution of pyridoxal phosphate and L-aspartic acid showing the aldehyde proton resonance of pyridoxal phosphate at 10.45 ppm and the carbon-bound imine proton resonance of the aldimine intermediate at 8.92 ppm. The carbon-bound imine proton resonance is well separated from other peaks and was therefore selected for the T_1 experiments.*

after mixing 6 mM L-Asp and 1.5 mM pyridoxal phosphate, with observation of the usual experimental precautions for accurate integration. The dissociation constant for dissociation of the aldimine to form pyridoxal phosphate and aspartic acid was estimated to be approximately 15 mM. The chemical shift of the methylene group of pyridoxamine phosphate at pH 7 was 4.33 ppm.

Circular dichroism spectroscopic evidence for aldimine – protein interactions

The interactions between the aldimine and the polypeptides T-4 and T-16 were monitored by CD spectroscopy according to the assumption that the formation of an aldimine – polypeptide complex would stabilise the folded structure. This assumption was borne out in practice as an increase in the helical content of both peptides was observed upon addition of the aldimine. The mean residue ellipticity of T-4 (0.75 mM) at 222 nm in 2-[4-(2-hydroxyethyl)-1-piperazinyl]ethanesulfonic acid (HEPES) buffer solution (100 mM) at room temperature and pH 7.4 was $-18\,500 \pm 500$ deg cm^2 dmol^{-1} (Table 1). Upon addition of L-as-

Table 1. *The mean residue ellipticities at 222 nm, Θ_{222}, of T-4 (0.5 mM) in the presence of pyridoxal phosphate (1.5 mM), L-aspartic acid (6 mM) or a mixture of pyridoxal phosphate (1.5 mM) and L-aspartic acid (6 mM) in aqueous solution at pH 7.4 and room temperature.*

Sample	$[\Theta]_{222}$ [deg cm^2 dmol^{-1}]
T-4	$-18\,500$
T-4 + L-Asp	$-18\,700$
T-4 + PLP	$-18\,500$
T-4 + (L-Asp + PLP)	$-19\,900$

partic acid (6 mM) or pyridoxal phosphate (1.5 mM) to the peptide solution (0.5 mM); the mean residue ellipticities at 222 nm were $-18\,700 \pm 500$ deg cm^2 dmol^{-1} and $-18\,500 \pm 500$ deg cm^2 dmol^{-1}, respectively. In contrast, when a mixture of L-aspartic acid (6 mM) and pyridoxal phosphate (1.5 mM) was added, the value of the mean residue ellipticity at 222 nm was $-19\,900 \pm 500$ deg cm^2 dmol^{-1}, which suggests that stabilisation of the secondary structure occurs upon introduction of the aldimine intermediate.

The mean residue ellipticity at 222 nm of T-16 (0.5 mM) in phosphate buffer solution (100 mM) at room temperature and pH 7.5 was $-21\,200 \pm 500$ deg cm^2 dmol^{-1} (Table 2). Addition of L-aspartic acid (10 mM) left the mean residue ellipticity at 222 nm unchanged, within experimental error, at $-21\,500 \pm 500$ deg cm^2 dmol^{-1}. Upon addition of pyridoxal phosphate (2.5 mM) to the peptide solution the value of the mean residue ellipticity at 222 nm became $-22\,800 \pm 500$ deg cm^2 dmol^{-1}. The addition of a mixture of L-aspartic acid (10 mM) and pyridoxal phosphate (2.5 mM) to the peptide solution increased the helicity considerably as the negative value of the mean residue ellipticity at 222 nm was increased to $-24\,000 \pm 500$ deg cm^2 dmol^{-1}. Significant stabilisation of the structure due to the noncovalent interactions between the peptide and the aldimine was

Table 2. *The mean residue ellipticities at 222 nm, Θ_{222}, of T-16 (0.5 mM) in the presence of pyridoxal phosphate (1.5 mM), L-aspartic acid (6 mM) or a mixture of pyridoxal phosphate (1.5 mM) and L-aspartic acid (6 mM) in aqueous solution at pH 7.5 and room temperature.*

Sample	$[\Theta]_{222}$ [deg cm^2 dmol^{-1}]
T-16	$-21\,200$
T-16 + L-Asp	$-21\,500$
T-16 + PLP	$-22\,800$
T-16 + (L-Asp + PLP)	$-24\,000$

established. For comparison, THref, which also folded into a helix-loop-helix dimer motif and included arginine and histidine residues, showed no increase in helical content after addition of pyridoxal phosphate, L-aspartic acid or a mixture of pyridoxal phosphate and L-aspartic acid under the conditions described above.

^{1}H NMR spectroscopy spin – lattice relaxation time measurements of aldimine – polypeptide interactions

The chemical shifts of the aldimine were only marginally affected by the addition of protein, which suggests that they are similar for the free and bound forms, or that the equilibrium concentration of bound aldimine is small. The interactions between the aldimine intermediate and the polypeptides T-4 and T-16 were therefore studied by measurement of the ^{1}H NMR spin – lattice relaxation time (T_1) of the imine proton of the aldimine. An effect on the T_1 value was expected if the aldimine was bound to the folded four-helix bundle and in fast exchange on the NMR time scale between the free and the bound state. This was indeed the case, as there were significant changes in the T_1 value of the imine proton in the presence of T-4 and T-16, in comparison with the corresponding value of the free aldimine. The measurements were carried out by using the inversion-recovery $(180^\circ - \tau - 90^\circ - t)_n$ pulse sequence with a nonselective 180° pulse as well as a selective Gaussian 180° pulse applied to the carbon-bound imine proton of the aldimine at 8.92 ppm. The imine proton resonance is well separated from other peaks and not obscured by resonances from amide protons or His or Phe ring protons of the peptide. Selective and nonselective measurements were obtained at 288, 298 and 308 K and the results are shown in Table 3 and Table 4. The T_1 value of the imine proton was affected by the presence of T-4 as well as by that of T-16, which demonstrates that the rotational correlation time of the aldimine was affected by the folded polypeptides and clearly establishes interactions with the four-helix bundles.

^{31}P NMR measurements of aldimine – polypeptide interactions

^{31}P NMR spectroscopic measurements were undertaken to further probe the interaction between the aldimine and the T-4 binding site. The resonance of the aldimine shifted by approximately 10 Hz, less than 0.1 ppm, upon addition of 3 mM T-4, which shows that the aldimine was bound by the polypeptide. However, the small shifts again suggested that measure-

Table 3. *^{1}H NMR spin – lattice (T_1) relaxation time measurements of the free aldimine intermediate in solution and of the intermediate in the presence of T-4.*[a]

| T-4 + PLP + L-Asp	T_1 (288 K)	T_1 (298 K)	T_1 (308 K)
selective	0.24	0.22	0.14
nonselective	0.22	0.21	0.14
PLP + L-Asp	T_1 (288 K)	T_1 (298 K)	T_1 (308 K)
selective	0.52	0.48	0.41
nonselective	0.53	0.46	0.40

[a] The measurements were performed in HEPES buffer (40 mM)/D$_2$O (90:10) at pH 7.4, at a peptide concentration of 0.75 mM and in the presence of pyridoxal phosphate (1.5 mM) and L-aspartic acid (6 mM).

Table 4. *^{1}H NMR spin – lattice (T_1) relaxation time measurements of the free aldimine intermediate in solution and of the intermediate in the presence of T-16.*[a]

T-16 + PLP + L-Asp	T_1 (288 K)	T_1 (298 K)	T_1 (308 K)
selective	0.72	0.65	0.57
nonselective	0.75	0.70	0.64
PLP + L-Asp	T_1 (288 K)	T_1 (298 K)	T_1 (308 K)
selective	0.47	0.46	0.43
nonselective	0.49	0.46	0.43

[a] The measurements were performed in phosphate buffer (100 mM)/D$_2$O (90:10) at pH 7.5 at a peptide concentration of 0.75 mM and in the presence of pyridoxal phosphate (1.5 mM) and L-aspartic acid (6 mM).

ment of the effects on relaxation would be more informative. The relaxation mechanism of the ^{31}P nucleus is predominantly a result of chemical shift anisotropy and binding of the aldimine to a macromolecule was expected to affect its relaxation properties in a detectable way. A solution of pyridoxal phosphate (7.5 mM) and L-aspartic acid (30 mM) in a 90:10 mixture of HEPES buffer (100 mM) and D$_2$O at pH 7.4 and 298 K was titrated with T-4
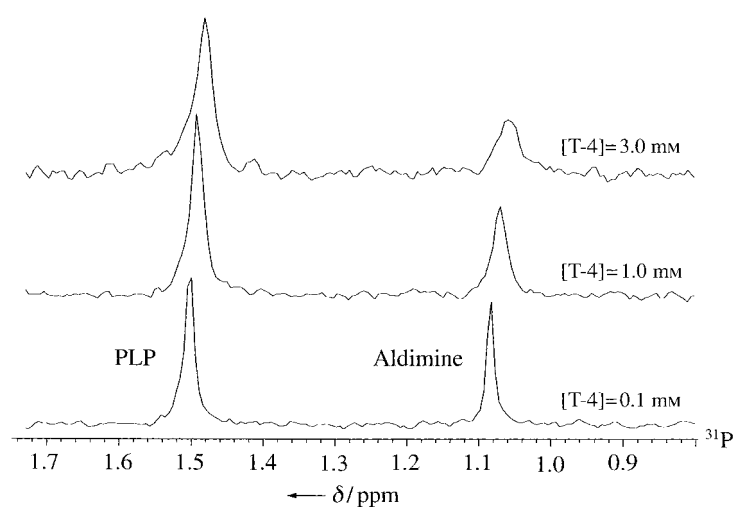
Figure 8. *The ^{31}P NMR spectrum of an aqueous solution of pyridoxal phosphate (7.5 mM) and L-aspartic acid (30 mM) upon titration with T-4. The increased line width of the aldimine resonance is caused by the increased correlation time that results from binding.*

(0.1 – 3.0 mM) to a final concentration of 3.0 mM. The ^{31}P NMR spectrum was recorded for each addition and the chemical shifts were recorded relative to an external reference consisting of 22 mM sodium phosphate at pH 7. The resonance at 1.53 ppm (Figure 8) is that of pyridoxal phosphate and upon addition of L-aspartic acid the aldimine phosphate resonance emerged at 1.10 ppm. The addition of T-4 to the pyridoxal phosphate and L-aspartic acid solution caused the linewidths of the pyridoxal phosphate and the aldimine resonances to increase, with the increase more pronounced for the aldimine. The increased line width of the aldimine resonance in the presence of the polypeptide is evidence for an increased correlation time that results from binding to the macromolecule.

Kinetic measurements by UV spectroscopy

While binding was clearly demonstrated by NMR and CD spectroscopies, the site of binding could not be established by these measurements. The most sensitive demonstration of specific binding of the aldimine to the designated binding sites would be the onset of catalysis, therefore the catalytic efficiencies of the folded polypeptides were determined by UV and NMR spectroscopies. The reactivities of the twenty-five designed helix-loop-helix dimers were screened by measuring the initial rates of pyridoxamine phosphate formation by following the increase in absorbance at 325 nm as a function of time by UV spectroscopy at 298 K. The measurements were carried out with 10 mM L-aspartic acid, 2.5 mM pyridoxal phosphate and peptide concentrations of 0.5 mM. The screening reactions were carried out at pH 6.0 and 7.4 for the histidine-containing peptides, and at pH 7.4 and 9.0 for the lysine-containing peptides. Little catalysis was observed in the presence of lysine-containing sequences, most likely because lysine residues form imines with the cofactor PLP, as described above. T-4 and T-16 were the most efficient c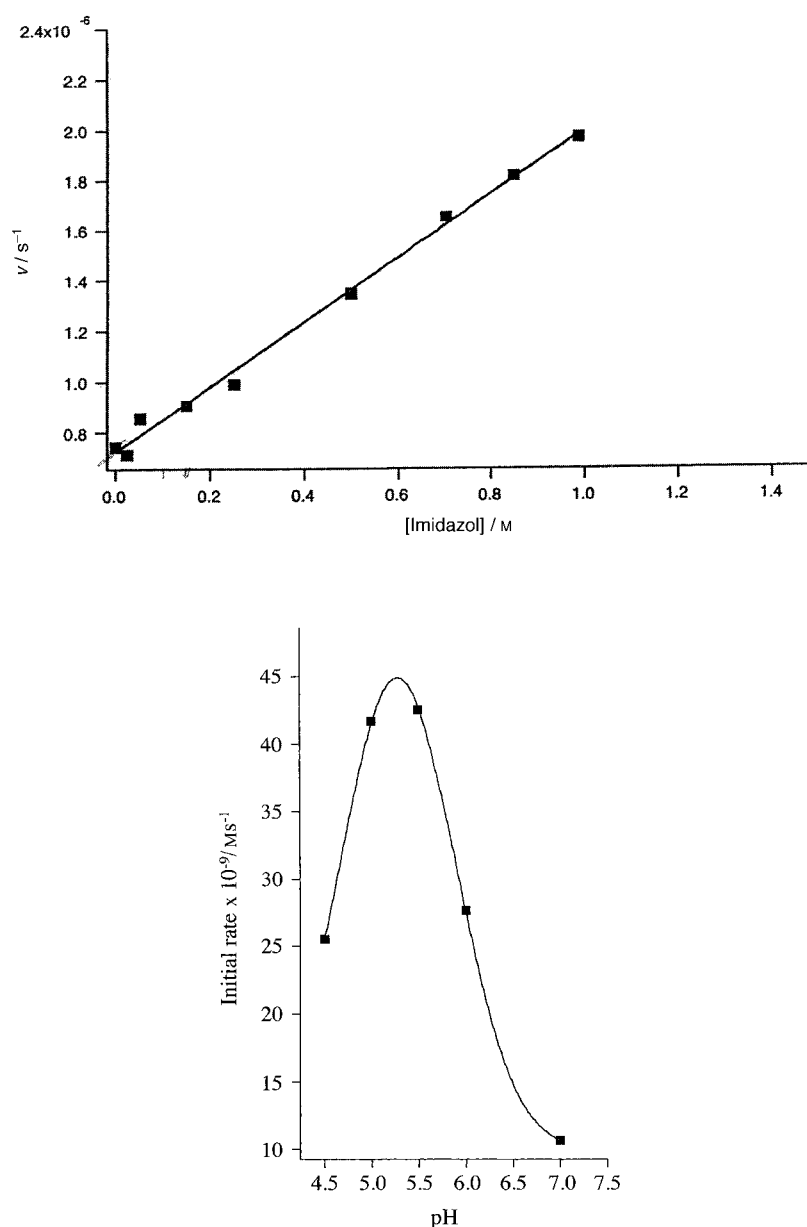atalysts and were therefore selected from the pool of sequences for further studies of the aldimine – polypeptide interactions. Attempts to determine whether they followed saturation kinetics failed, probably because the high concentrations of L-Asp and pyridoxal phosphate needed to generate sufficient concentrations of aldimine affected the structures of the catalysts. The equilibrium constant of 15 mM for the dissociation of the aldimine to form L-Asp and PLP makes it necessary to use concentrations of L-Asp as high as 150 mM, in combination with 16 mM PLP to generate the 15 mM aldimine required to determine K_M values in the millimolar range. The accessible concentration range of PLP is limited by its poor solubility. The T-16-catalysed reaction appeared to follow saturation kinetics when L-Asp concentration was varied at a constant PLP concentration of 8 mM, but not when the PLP concentration was varied at a constant L-Asp concentration of 100 mM. These experiments were carried out in 100 mM phosphate buffer with 0.15 M NaCl added to minimise variations in ionic strength. The complexity of the transamination reaction and the high concentrations of substrates needed were likely to make

these measurements difficult to analyse. Instead, a comparison between imidazole, T-4 and T-16 was carried out under experimental conditions for which no kinetic model was assumed. The rates were relative measurements of initial rates obtained from the slopes of absorbance versus time, obtained under identical buffer and reagent concentration, and pH and temperature conditions. Initial rates of pyridoxamine phosphate formation were determined at 0.5 mM peptide, 2.5 mM PLP and 10 mM L-Asp, pH 5.5 and 288 K, and compared to the corresponding rates for the imidazole-catalysed reaction. The initial rates under these conditions were 1.4×10^{-6} s^{-1} for the T-4-catalysed reaction and 2.2×10^{-6} s^{-1} for the T-16-catalysed reaction. Addition of 540 mM imidazole was required to obtain the initial rate of pyridoxamine phosphate formation observed in the presence of 0.5 mM T-4, (Figure 9) and the catalytic efficiency of T-4 was thus more than three orders of magnitude larger than that of imidazole. An imidazole concentration of 1.2 M was needed to match the catalytic efficiency of T-16, which indicates that the efficiency of T-16 is 2.4×10^3 times larger than that of imidazole. The pH value of 5.5 was chosen in an attempt to optimise the conditions for stabilisation of the transition state in the rate-limiting 1,3 proton transfer reaction. At pH 5.5, the pyridinium ion is expected to be formed to a large extent, and the concentration of protonated and unprotonated His residues should be close to optimal. Further support for the conclusion that the His residues are responsible for the 1,3 proton transfer reaction was provided by the pH profile of the transamination reaction, which was determined by measurements of T-16-catalysed transamination rates as a function of pH. T-16 (0.5 mM) was used to catalyse the transamination of the aldimine generated from 8.0 mM PLP and 150 mM L-Asp in 100 mM phosphate buffer containing 0.15 M NaCl at 288 K. The observed pH dependence did not fit with the pK_a value of the aldimine pyridinium ion but did fit with that of the His residues of the catalyst (Figure 9).

Figure 9. *a) Initial rates (absorbance versus time) of imidazole-catalysed transamination of L-Asp to form oxaloacetate, versus imidazole concentration in phosphate buffer (100 mM) at pH 5.5 and 288 K. The concentration of PLP was 2.5 mM and that of L-Asp was 10 mM. b) The pH profile of initial rates of T-16-catalysed transamination of L-Asp to form oxaloacetate. The concentration of T-16 was 0.5 mM, that of PLP was 8.0 mM and that of L-Asp was 150 mM. The reactions were carried out at 288 K in phosphate buffer (100 mM) containing NaCl (0.15 M). Initial rates were computed from absorbance versus time plots by using an extinction coefficient of 8372 M^{-1} cm^{-1}.*

Kinetic measurements by ^{1}H NMR spectroscopy

The reactivities of T-4 and T-16 were also followed by ^{1}H NMR spectroscopy by calculating the initial rates of pyridoxamine phosphate formation from the increase in intensity of the resonance of the methylene protons at 4.33 ppm as a function of time. The kinetic measurements were performed at 298 K in the presence of 10 mM L-aspartic acid, 2.5 mM pyridoxal phosphate and 0.5 mM peptide at pH 6.0 and 7.4. These measurements were

made to ensure that pyridoxamine phosphate was formed in the course of the reaction measured by UV spectroscopy.

Discussion

The rational design of binding sites for small molecules in aqueous solution is an important endeavour because it tests our understanding of biomolecular recognition and interactions, and because there are many applications in the field of biomedical and biotechnological research. The difficulties are mainly caused

by the fact that the binding energies that arise from interactions between a receptor and a ligand are small in aqueous solution because of the complex solvation phenomena involving the binding residues. In addition, interactions between proteins and small compounds are inherently weak as a result of the limited number of functional groups and the small contact area involved, and multiple interactions of high precision are required to provide sufficient overall affinity. Efficient binding of small molecules is nevertheless common in nature; binding sites are specifically tailored for their purpose and enzymes bind substrates, transition states and intermediates with high and differential affinity. Our understanding of protein structure has not yet reached a level where several functional groups can be positioned in geometrical relationships by rational design with a precision that mimics the fine-tuned active sites of enzymes. The design of a binding site in a four-helix bundle model protein was undertaken to further our understanding of the requirements for recognition and binding of the aldimine, and to construct a binding site for catalysis of the transamination reaction.

The design was based on the fact that aldimine is a highly negatively charged species, and that a four-helix bundle with multiple positive charges, that is, with several arginine residues, should be the starting point in the search for optimum recognition and binding. The sequence of T-16 contains six Asp or Glu residues, seven Arg residues and two His residues, which gives a total charge at approximately neutral pH of $+1$ to $+2$. T-4 contained five Asp or Glu residues, five Arg residues and five His residues. The design of a binding site based mainly on charge–charge interactions requires several cooperative binding interactions since the free energy of salt-bridge formation is small. For comparison, the free energy of dissociation of a solvent-exposed Glu–Lys salt bridge has been reported to be 0.5 kcal mol^{-1}.[11] In catalysis, the transition state along the reaction coordinate should be bound strongly, whereas substrates and low-energy intermediates should be bound with only modest affinities. Since we attempted to construct only moderately efficient binding sites, the detection strategies used had to be carefully considered. The transamination reaction is most often studied by UV spectroscopy; the cofactor pyridoxal phosphate absorbs at 389 nm and pyridoxamine phosphate absorbs at 325 nm.[35] The absorbtion maxima of the intermediates remain, unfortunately, to be unequivocally assigned and various suggestions have been reported.[35, 51, 53–57] UV spectroscopy was therefore not used to study the binding of the intermediates. Instead CD and NMR spectroscopic techniques were employed.

The CD spectrum of a polypeptide provides a measure of its secondary structure. Since binding of the aldimine to the designed binding sites was expected to stabilise the folded four-helix bundles, the CD spectra of T-4, T-16 and THref were recorded in the presence of L-Asp, pyridoxal phosphate and a mixture of both. T-4 and T-16 showed increasingly negative mean residue ellipticities at 222 nm upon addition of the aldimine intermediate (Tables 1 and 2), which provided strong evidence for binding. For T-16, some stabilisation was obtained by the addition of only the pyridoxal phosphate cofactor. This is not surprising as pyridoxal phosphate is part of the aldimine

moiety and some interaction between the cofactor and the polypeptide was to be expected. Upon addition of the aldimine to T-16, stabilisation of the structure was observed as a change in mean residue ellipticity from $-21\,200$ to $-24\,000$ deg cm^2 dmol^{-1}. Although part of the change was due to the interaction with the cofactor, this observation shows significant stabilisation of the structure by noncovalent interaction between the aldimine and the polypeptide scaffold. An equilibrium constant could not be determined from the experimental data because the mean residue ellipticity of the T-16–aldimine complex could not be obtained. Nevertheless, an increase in helicity of more than 10% suggested that a large fraction of the total concentration of T-16 was involved in a complex with the aldimine because unrealistic values of the mean residue ellipticity of the complex would otherwise have to be assumed. The mean residue ellipticity of T-16 in the absence of aldimine ($-21\,200$ deg cm^2 dmol^{-1}) was within the range of most four-helix bundle structures in the SA-42 series of sequences. The largest negative value measured for any of the sequences was $-26\,000$ deg cm^2 dmol^{-1}. An order-of-magnitude calculation therefore indicates that no less than 20%, and probably more, of the T-16 was complexed by the aldimine. The dissociation constant of the T-16–aldimine complex was estimated very approximately to be in the millimolar range by using the estimated value of the dissociation constant of the aldimine (15 mM) and the experimental concentrations of T-16 (0.5 mM), L-Asp (2.5 mM) and pyridoxal phosphate (10 mM). The mean residue ellipticity of the reference peptide THref was unaffected by the addition of L-Asp, the cofactor or a mixture of the two. The interactions between the binding sites and the aldimine are therefore specific and not due to salt effects on polypeptide structure.

Further insights into the interactions were obtained from the ^{1}H NMR spectrum of the aldimine and of the aldimine in the presence of the polypeptides. The interactions between the aldimine and the polypeptide scaffolds were not strong enough to give rise to separate resonances for free and bound aldimine. The exchange between the free and the bound states was fast on the NMR time scale and the observed resonances of the aldimine were the weighted averages and did not provide detailed structural information about the complex. The chemical shifts were only affected to a small degree by the addition of the polypeptides, although these small changes demonstrated the presence of interactions between the polypeptides and the aldimine. Since the effects on the mean residue ellipticities suggested that the interactions were significant, we concluded that the chemical shifts do not change much upon binding. A probable explanation is that several binding conformations are populated, with the result that an averaged chemical shift close to that of the free aldimine is observed. Relaxation time measurements were instead used to establish the binding of the intermediate since relaxation times depend on the rotational correlation time of the nuclei and therefore on molecular size.[52, 58, 59] The sequences consist of 42 residues with molecular weights of approximately 4700. The weight of the dimer, which is the predominant species in solution at 0.75 mM, is 9400. As there is a considerable difference in molecular weight between

the aldimine (360 g mol^{-1}) and the aldimine–polypeptide complex, the longitudinal relaxation time, T_1, of the aldimine intermediate was expected to be sensitive to the formation of the complex and this was found to be the case. The T_1 value of the imine CH proton of the free aldimine, found by using a nonselective as well as a selective pulse sequence, was 0.5 s in aqueous solution at pH 7.5 and 288 K. In the presence of T-16, the T_1 value of the CH proton increased to 0.7 s, whereas this value was reduced to 0.2 s in the presence of T-4. The relative magnitudes depend on the binding constants as well as on the molecular weights of the protein receptors, but are also influenced by the dynamics of the binding site. Free aldimine in the absence of the polypeptide tumbles rapidly and is characterised by short rotational correlation times. When the aldimine is bound to T-4 or T-16, the rotational correlation time changes to that of the macromolecule and under conditions of fast exchange between the free and bound states, the effective relaxation is influenced by the residence times and by the dynamics in the bound state. The difference in the T_1 value between free and bound aldimine demonstrates that there is an interaction between the two components, even if it cannot be quantified. The absolute value of the change in T_1 has little quantitative meaning since dynamics in the binding site may affect the effective rotational correlation time. An increase as well as a decrease in the T_1 value may therefore result from complexation of a small molecule by a protein.

The ^{31}P NMR spectrum of the aldimine was also informative with regards to peptide–aldimine interactions. The linewidth of the ^{31}P NMR resonance of the aldimine at 1.10 ppm increased in the presence of peptide T-4, as did that of the pyridoxal phosphate resonance at 1.53 ppm, although the increase in linewidth of the aldimine resonance was larger. The increased line width of the aldimine resonance is a measure of a reduced T_2 value and is due to the increased rotational correlation time that results from binding of the aldimine and cofactor to the macromolecule (Figure 7).[52, 59]

While the CD and NMR spectroscopic measurements provided clear evidence for binding, the small chemical shifts provided little guidance in determining the nature and location of the binding site. Kinetic measurements were instead used to probe whether the intermediate was bound in close proximity to the His residues. The transformation of the aldimine to the ketimine, which was monitored by measuring the rate of appearance of pyridoxamine phosphate, requires a proton-transfer reaction that can only be catalysed by a general acid or a general base or a combination of the two. T-4 and T-16 emerged as catalytically active polypeptides from the pool of sequences designed to bind the aldimine and since there are no lysine residues in the sequences of T-4 and T-16, we concluded that the His residues were the catalytically active side chains. A comparison between initial rates of pyridoxamine phosphate formation catalysed by T-4, T-16 or imidazole showed that the polypeptides were more than three orders of magnitude more efficient than imidazole at catalysing the reaction. These results provide strong evidence for close proximity between the CH protons of the aldimine and the histidine residues of the catalyst. A rate enhancement of more than three orders of magnitude is not compatible with a simple

bimolecular reaction in solution catalysed by solvent-exposed His residues; polypeptide sequences with His residues other than those of T-4 and T-16 showed lower or no catalytic activity. Several of the sequences did not show any detectable catalytic efficiency although they contained Arg as well as His residues. The demonstration of aldimine binding by T-4 and T-16 in the millimolar range, in combination with the efficient catalytic activity seen, therefore demonstrates that the reaction takes place in the designed binding sites. It is not likely that the rate enhancement in the imidazole-catalysed reaction is an effect of the increased ionic strength resulting from the high concentration of imidazolium ion. The plot of reaction rate v against [Im] is linear and the ionic strength resulting from 100 mM phosphate buffer is high, even at low imidazole concentration. However, if the increased ionic strength were to have an effect, then the relative rate enhancements achieved by the polypeptide catalysts would be even higher.

Conclusion

Binding sites for aldimine intermediates have been designed for the purpose of catalysing the transformation of aldimine into ketimine in the pathway of the biosynthesis of amino acids. The binding sites were designed to interact with the aldimine mainly through noncovalent charge–charge interactions between positively charged residues in the folded polypeptide and the negatively charged substituents of the aldimine. The binding sites were also equipped with His residues capable of catalysing the rate-limiting 1,3 proton transfer step of the transamination reaction. The design of the binding sites was successful; catalysts T-4 and T-16 were capable of binding the aldimines with millimolar affinity and catalyse the reaction in the reactive site with an efficiency more than three orders of magnitude larger than that of imidazole.

Experimental

Peptide synthesis, purification and identification: The polypeptides were synthesised on an automated peptide synthesiser (Pioneer, Applied Biosystems) by using 9-fluorenylmethoxycarbonyl (Fmoc) protection group strategies. The syntheses were performed on a 0.1-mmol scale and the Fmoc-protected amino acids were activated in situ by treatment with *O*-(7-benzotriazole-1-yl)-1,1,3,3-tetramethyluronium tetrafluoroborate (TBTU; 0.5 M in dimethylformamide (DMF)) and diisopropylethylamine (DIPEA; 1.0 M in DMF). The Fmoc protection groups were removed by treatment with piperidine (20 % v/v in DMF). The side-chain protection groups were *tert*-butoxy (O*t*Bu) for Asp and Glu, trityl (Trt) for His, Asn and Gln, *tert*-butoxycarbonyl (*t*Boc) for Lys, *tert*-butyl (*t*Bu) for Tyr and 2,2,4,6,7-pentamethyldihydrobenzofuran-5-sulfonyl (Pbf) for Arg. Coupling times were 60 minutes, except for Arg and difficult parts in the sequence where 90-minute times were used. The amino terminal was capped with acetic anhydride (0.3 M in DMF). The carboxy terminal was amidated upon cleavage from the resin by using a 5-(aminomethyl-3,5-dimethoxyphenoxy)valeric acid linked polyethyleneglycol spacer on a polystyrene polymer support (Applied Biosystems) with a substitution level of 0.18–0.22 mmol g^{-1}. The peptides were cleaved from the resin and deprotected by treatment

with a mixture containing trifluoroacetic acid (TFA)/H$_2$O/ethanedithiol/triisopropylsilane (94:2.5:2.5:1) (20 mL g^{-1}) for two hours at room temperature. After filtration and concentration of the mixture, the peptides were precipitated by addition of cold diethyl ether, centrifuged and lyophilised. The peptides were purified by reversed-phase HPLC on a semipreparative C-8 column (HICHROM) and eluted isocratically with propan-2-ol (34% for T-4 and 33% for T-16, v/v) in TFA (0.1%, v/v) at a flow rate of 8 mL min^{-1}, followed by UV detection at 229 nm. The purity of each peptide was determined by reversed-phase analytical HPLC. No peak other than that of the desired peptide was present in the chromatograms after purification. The identities of the peptides were determined by ESI MS on a magnetic sector spectrometer (VG ZabSpec). The obtained molecular weight was within 1 a.u. of the calculated value and no high-molecular-weight impurities could be detected.

^{1}H NMR spectroscopy: The ^{1}H NMR spectra were recorded on a Varian Inova 600-MHz NMR spectrometer. The concentrations of T-4 and T-16 in the solutions were estimated by weight, assuming a water content of 30%, and subsequently determined by quantitative amino acid analysis. Pyridoxal phosphate and L-aspartic acid were purchased from Sigma – Aldrich and used as supplied. The solutions for determining the T_1 value of the aldimine in the presence of T-4 were prepared in HEPES buffer (40 mM)/D$_2$O (90:10) solution and contained T-4 (0.75 mM), pyridoxal phosphate (1.5 mM) and L-Asp (6 mM). The measurements were performed at pH 7.4 and at 288, 298 and 308 K. The pH value was adjusted with HCl and NaOH and the solutions were carefully deoxygenated by purging with nitrogen gas. Solutions for determining relaxation rates in the presence of T-16 were prepared in phosphate buffer (100 mM)/D$_2$O (90:10) solution and contained T-16 (0.75 mM), pyridoxal phosphate (1.5 mM) and L-Asp (6 mM). The measurements were performed at pH 7.5 and at 288, 298 and 308 K. The pH value was adjusted with HCl and NaOH and the solutions were carefully deoxygenated by purging with nitrogen gas.

Spin – lattice relaxation times of the carbon-bound imine proton at 8.92 ppm were measured by using the $(180° - \tau - 90° - t)_n$ pulse sequence. The τ values for the selective and nonselective experiments were: 0, 0.05, 0.1, 0.15, 0.2, 0.25, 0.3, 0.35, 0.4, 0.45, 0.5, 0.55, 0.6, 0.65, 0.7, 0.8, 0.9, 1.0, 1.2, 1.5, 1.8, 2.0, 2.5, 3.0, 4.0, 6.0 and 8.0 seconds. For the selective experiments a Gaussian 180° pulse was generated by using the Varian pulse sequence sh2pul, modified to include presaturation. The selective spin – lattice relaxation rates were calculated with standard Varian software. The maximum experimental error in the relaxation rate measurements was ± 0.1 s.

Kinetic measurements of pyridoxamine phosphate formation were carried out under the following experimental conditions: 0.5 mM T-4 or T-16 at pH 7.4 and 6.0, at 298 K, in the presence of L-Asp (10 mM) and pyridoxal phosphate (2.5 mM) in aqueous buffer solution/D$_2$O (90:10).

^{31}P NMR spectroscopy: The ^{31}P NMR spectra were recorded on a 400-MHz Varian Unity NMR spectrometer at pH 7.4 and 298 K. The solutions were prepared in HEPES buffer (100 mM)/D$_2$O (90:10) and the pH value was adjusted with HCl and NaOH. T-4 was added in portions (0.1 – 3.0 mM) to the pyridoxal phosphate (7.5 mM) and L-aspartic acid (30 mM) solution. A potassium phosphate solution (22 mM; pH 7) was used as an external standard.

Circular dichroism spectroscopy: CD spectra were recorded on a Jasco J-720 spectropolarimeter, routinely calibrated with D-(+)-camphor-10-sulfonic acid. The spectra were measured at room temperature in the wavelength interval 280 – 190 nm in 0.1- or 0.5-mm cuvettes. The peptide concentrations were estimated by weight, assuming a water content of 30%, and subsequently determined by

quantitative amino acid analysis. Stock solutions of T-4, T-16, L-aspartic acid and pyridoxal phosphate were used for accuracy.

Kinetic measurements by UV spectroscopy: The kinetic experiments were carried out with spectrophotometers (Varian Cary 1 or 5) equipped with temperature controllers (Varian). Initial rates were determined by measuring the absorbance at 325 nm as a function of time with a peptide concentration of 0.5 mM, a pyridoxal phosphate concentration of 2.5 mM and an L-aspartic acid concentration of 10 mM. The extinction coefficient at 325 nm was 8372 M^{-1} cm^{-1}. Stock solutions of peptides, pyridoxal phosphate, L-aspartic acid and imidazole were prepared in phosphate buffer solution (100 mM) and the pH value was adjusted when necessary to 5.5, 6.0, 7.4 or 9.0. The concentrations of the peptide stock solutions were determined by quantitative amino acid analysis. In a typical kinetic experiment, 275 μL solution was used in a 1-mm quartz cuvette. The peptide and L-aspartic acid solution was temperature equilibrated for at least 30 minutes before addition of the pyridoxal phosphate solution. The measurements were started after brief shaking of the cuvette and re-introduction into the thermostated cell compartment and the reactions were followed for five hours. The initial rates were determined by fitting the equation for a straight line to the experimental data.

The initial rates at different imidazole concentrations (0 – 1.0 M) were determined under the same reaction conditions as described above.

The initial rates as a function of pH value were determined at 0.5 mM T-16, 8.0 mM PLP and 150 mM L-Asp in phosphate buffer (100 mM) containing NaCl (0.15 M) at 288 K.

[1] K. Johnsson, R. K. Allemann, H. Widmer, S. A. Benner, *Nature* **1993**, *365*, 530.
[2] L. Baltzer, J. Nilsson, *Curr. Opin. Biotechnol.* **2001**, *12*, 355.
[3] R. B. Hill, D. P. Raleigh, A. Lombardi, W. F. DeGrado, *Acc. Chem. Res.* **2000**, *33*, 745.
[4] P. G. Schultz, R. A. Lerner, *Science* **1995**, *269*, 1835.
[5] C. F. Barbas III, A. Heine, G. Zhong, T. Hoffmann, S. Gramatikova, R. Bjornestedt, B. List, J. Anderson, E. A. Stura, I. A. Wilson, R. A. Lerner, *Science* **1997**, *278*, 2085.
[6] T. Hoffmann, G. Zhong, B. List, D. Shabat, J. Anderson, S. Gramatikova, R. A. Lerner, C. F. Barbas III, *J. Am. Chem. Soc.* **1998**, *120*, 2768.
[7] J. D. Stevenson, N. R. Thomas, *Nat. Prod. Rep.* **2000**, *17*, 535.
[8] T. M. Penning, J. M. Jez, *Chem. Rev.* **2001**, *101*, 3027.
[9] D. Qi, C.-M. Tann, D. Haring, M. D. Distefano, *Chem. Rev.* **2001**, *101*, 3081.
[10] M. Mutter, G. G. Tuchscherer, C. Miller, K.-H. Altmann, R. I. Carey, D. F. Wyss, A. M. Labhardt, J. E. Rivier, *J. Am. Chem. Soc.* **1992**, *114*, 1463.
[11] J. W. Bryson, S. F. Betz, H. S. Lu, D. J. Suich, H. X. Zhou, K. T. O'Neil, W. F. DeGrado, *Science* **1995**, *270*, 935.
[12] S. Kamtekar, M. H. Hecht, *FASEB J.* **1995**, *9*, 1013.
[13] M. D. Struthers, R. P. Cheng, B. Imperiali, *Science* **1996**, *271*, 342.
[14] C. E. Schafmeister, R. M. Stroud, *Curr. Opin. Biotechnol.* **1998**, *9*, 350.
[15] W. D. Kohn, R. S. Hodges, *Trends Biotechnol.* **1998**, *16*, 379.
[16] E. Lacroix, T. Kortemme, M. Lopez del la Paz, L. Serrano, *Curr. Opin. Struct. Biol.* **1999**, *9*, 487.
[17] W. F. DeGrado, C. M. Summa, V. Pavone, F. Nastri, A. Lombardi, *Annu. Rev. Biochem.* **1999**, *68*, 779.
[18] L. Baltzer, H. Nilsson, J. Nilsson, *Chem. Rev.* **2001**, *101*, 3153.

[19] C. Smith, L. Regan, *Acc. Chem. Res.* **1997**, *30*, 153.

[20] M. S. Searle, *J. Chem. Soc. Perkin Trans. 2* **2001**, *7*, 1011.

[21] M. Allert, M. Kjellstrand, K. Broo, A. Nilsson, L. Baltzer, *J. Chem. Soc. Perkin Trans. 2* **1998**, 2271.

[22] M. Allert, L. Baltzer, *Chem. Eur. J.* **2002**, 2549.

[23] D. H. Lee, J. R. Granja, J. A. Martinez, K. Severin, R. M. Ghadiri, *Nature* **1996**, *382*, 525.

[24] K. Severin, D. H. Lee, A. J. Kennan, R. M. Ghadiri, *Nature* **1997**, *389*, 706.

[25] S. Yao, I. Ghosh, R. Zutshi, J. Chmielewski, *J. Am. Chem. Soc.* **1997**, *119*, 10 559.

[26] S. Yao, I. Ghosh, R. Zutshi, J. Chmielewski, *Nature* **1998**, *396*, 447.

[27] A. J. Kennan, V. Haridas, K. Severin, D. H. Lee, R. M. Ghadiri, *J. Am. Chem. Soc.* **2001**, *123*, 1797.

[28] K. Broo, L. Brive, A.-C. Lundh, P. Ahlberg, L. Baltzer, *J. Am. Chem. Soc.* **1996**, *118*, 8172.

[29] K. S. Broo, L. Brive, P. Ahlberg, L. Baltzer, *J. Am. Chem. Soc.* **1997**, *119*, 11 362.

[30] K. S. Broo, H. Nilsson, J. Nilsson, L. Baltzer, *J. Am. Chem. Soc.* **1998**, *120*, 10 287.

[31] K. S. Broo, L. Brive, R. S. Sott, L. Baltzer, *Folding Des.* **1998**, *3*, 303.

[32] K. S. Broo, H. Nilsson, J. Nilsson, A. Flodberg, L. Baltzer, *J. Am. Chem. Soc.* **1998**, *120*, 4063.

[33] M. A. Shogren-Knaak, B. Imperiali, *Bioorg. Med. Chem.* **1999**, *7*, 1993.

[34] M. van Holde in *Biochemistry*, The Benjamine/Cummings Publishing Company, Redwood City, **1990**, p. 680.

[35] T. Bugg in *An Introduction to Enzyme and Coenzyme Chemistry*, Blackwell Science Ltd., London, **1997**, p. 185.

[36] A. Fersht in *Structure and Mechanism in Protein Science*, W. H. Freeman and Company, USA, **1999**, p. 79.

[37] H. Kuang, M. L. Brown, R. R. Davies, E. C. Young, M. D. Distefano, *J. Am. Chem. Soc.* **1996**, *118*, 10 702.

[38] H. Kuang, M. D. Distefano, *J. Am. Chem. Soc.* **1998**, *120*, 1072.

[39] D. Häring, M. D. Distefano, *Bioconjugate Chem.* **2001**, *12*, 385.

[40] R. Sinha Roy, B. Imperiali, *Protein Eng.* **1997**, *10*, 691.

[41] S. Olofsson, G. Johansson, L. Baltzer, *J. Chem. Soc. Perkin Trans. 2* **1995**, 2047.

[42] S. Olofsson, L. Baltzer, *Folding Des.* **1996**, *1*, 347.

[43] L. K. Andersson, G. T. Dolphin, J. Kihlberg, L. Baltzer, *J. Chem. Soc. Perkin Trans. 2* **2000**, 459.

[44] S. F. Betz, W. F. DeGrado, *Biochemistry* **1996**, *35*, 6955.

[45] L. K. Andersson, M. Caspersson, L. Baltzer, *Chem. Eur. J.* **2003**, in press.

[46] L. Baltzer, K. S. Broo, H. Nilsson, J. Nilsson, *Bioorg. Med. Chem.* **1999**, *7*, 83.

[47] M. Allert, Å. Nilsson, L. Baltzer, *J. Chem. Soc. Perkin Trans. 2*, submitted.

[48] R. A. John, *Biochim. Biophys. Acta* **1995**, *1248*, 81.

[49] H. Hayashi, *J. Biochem.* **1995**, *118*, 463.

[50] M. Allert, M. Kjellstrand, K. Broo, Å. Nilsson, L. Baltzer, *Chem. Commun.* **1998**, 1547.

[51] M. D. Toney, J. F. Kirsch, *Biochemistry* **1993**, *32*, 1471.

[52] K. A. Connors in *Binding Constants-The Measurement of Molecular Complex Stability*, John Wiley & Sons, New York, **1987**, p. 189.

[53] V. M. Malashkevich, M. D. Toney, J. N. Jansonius, *Biochemistry* **1993**, *32*, 13 451.

[54] T. Yano, S. Kuramitsu, S. Tanase, Y. Morino, H. Kagamiyama, *Biochemistry* **1992**, *31*, 5878.

[55] J. M. Goldberg, J. F. Kirsch, *Biochemistry* **1996**, *35*, 5280.

[56] D. Ringe, K. Soda, *Biochemistry* **1992**, *31*, 11 748.

[57] J. M. Goldberg, J. Zheng, H. Deng, Y. Q. Chen, R. Callender, J. F. Kirsch, *Biochemistry* **1993**, *32*, 8092.

[58] I. D. Campbell, R. Freeman, *J. Magn. Reson.* **1973**, *11*, 143.

[59] D. J. Craik, J. A. Wilce in *Protein NMR Techniques*, Reid, (Ed.: G. David), Humana Press Inc., Totowa, **1997**, p. 195.